Novel R-type Lectin Domain-Containing Cytotoxins Comprise a Family of Virulence-Modifying Proteins in Pathogenic *Leptospira*

Reetika Chaurasia,[1] Alan Marroquin,[1] Michael A. Matthias,[1*] and Joseph M. Vinetz[1*]

[1]Section of Infectious Diseases, Department of Internal Medicine, Yale University School of Medicine, New Haven, Connecticut 06520-8022, USA

[*]Correspondence to M.A.M (michael.matthias@yale.edu) or J.M.V. (joseph.vinetz@yale.edu)

Abstract

Leptospirosis is a globally important neglected zoonotic disease subject to both small scale outbreaks and weather-driven, large-scale epidemics. Due to gaps in our understanding of *Leptospira* biology, pathogenetic mechanisms of leptospirosis remain largely unknown. Previous data suggest that a gene family, PF07598, unique amongst most known bacterial pathogens and encoding so-called "Virulence-Modifying (VM)" proteins, are important virulence determinants. Here, we show that VM proteins are potent cytotoxins, sharing a distinct domain organization while exhibiting varied mechanisms of cellular toxicity. Structural homology searches using Phyre2 suggest that VM proteins are novel R-type lectins containing an N-terminal ricin B chain-like domain. As is known for native ricin B-chain, recombinant full-length **rLA3490** (most highly up-regulated *in vivo*) and an N-terminal fragment, **t3490**, containing a partial ricin B-domain, bound to asialofetuin and directly competed for asialofetuin binding with recombinant ricin B chain. While **t3490** bound to the HeLa cell surface but was neither internalized nor cytotoxic, **rLA3490** bound to the HeLa cell surface, was rapidly internalized, translocated to the nucleus inducing chromosomal fragmentation, and was rapidly cytolethal, providing strong evidence that *Leptospira* VM proteins are *bona fide* cytotoxins. Because monoclonal antibodies impeding cell entry or intracellular trafficking of ricin holotoxin clearly mitigate its toxicity, that VM proteins share binding and intracellular trafficking mechanisms suggests that anti-VM-protein antibody-based (anti-toxin) therapeutics could ameliorate severe complications of leptospirosis thereby improving prognosis. As most VM proteins are restricted to high-virulence *Leptospira* species with some, e.g., LA3490, being exceptionally potent, their level in serum might be a potentially useful indicator of a poor prognosis, thus identifying high risk patients.

Author Summary

The PF07598 gene family encoding Virulence-Modifying (VM) proteins in pathogenic *Leptospira* species is associated with severe manifestations of leptospirosis. Structural homology searches indicate that VM proteins contain an N-terminal ricin B chain-like domain, biochemically confirmed in asialofetuin binding and competitive-binding assays suggesting that VM proteins bind to terminal galactosyl residues of this model ricin B domain binding protein. The leptospiral N-terminal ricin B chain-like domain mediated VM protein binding to HeLa cells. Full-length recombinant protein rapidly led to cell death. Amino acid conservation among PF07598 family members at the N-terminal ricin B chain-like domain suggests that VM protein levels in serum might be a useful biomarker for quickly identifying at-risk patients, and that novel "anti-toxin"-based therapeutics could ameliorate severe complications of leptospirosis, both of which remain to be explored.

Keywords: cytotoxin, ricin B-like, lectin, genotoxin, cytopathic effect

Introduction

Leptospirosis is a globally important neglected zoonotic disease subject to both small scale outbreaks and weather-driven, large-scale epidemics, with substantial impact on veterinary and public health. Conservative estimates suggest that the global burden of human disease due to leptospirosis is on par with cholera and typhoid fever (1-3). Annually, more than 1 million cases and 58,900 deaths are estimated to occur globally with case fatality rates ranging from 5-20% (1, 4). Humans become infected after exposure to freshwater or wet soils contaminated by the urine of mammalian reservoir hosts. Clinical presentation varies from an undifferentiated fever to jaundice, renal failure, pulmonary hemorrhage, shock and fulminant death (5-10). Despite informative *in vitro* and small animal models, the molecular, cellular and immunological mechanisms of disease pathogenesis remain unclear (6, 11).

Previously published genomic, pathogenomic and gene expression data suggest that the PF07598 gene family, encoding the so-called Virulence Modifying (VM) proteins, may contribute to the pathogenesis of leptospirosis. VM proteins contain secretory signal peptides (12), and the expression of various PF07598 gene family members is upregulated, both in vitro, under conditions mimicking the in vivo host environment (13), and in vivo in small animal models of acute infection (14). That VM proteins are restricted to group I pathogenic *Leptospira* and expanded in the most highly pathogenic *Leptospira* species and serovars (12, 14), including the cosmopolitan and lethal serovars Copenhageni and Canicola, further suggests that they are involved in pathogenesis.

Based on structural homology searches using Phyre2 (15) that identified, with high confidence, an N-terminal R-type lectin (ricin B-like) domain in the PF07598 gene family, we hypothesized that VM proteins, like ricin, are cytotoxins. First, we tested whether the putative ricin

B-like domain in both recombinant full-length, and a truncated protein containing a (partial) ricin B domain of LA3490, the most highly up-regulated PF07598 gene in vivo (14), like ricin B chain, bound to immobilized asialofetuin, a terminal galactosyl-containing glycoprotein, in vitro (16, 17). Next, we determined whether recombinant full-length and truncated recombinant protein LA3490 produced cytopathic effects on cultured HeLa cells. A detailed comparative cross-serovar and cross-species computational analysis was done to assess potential therapeutic potential of anti-VM protein antibodies and biological plausibility of conserved VM protein ricin B domains as vaccine candidates.

Results

Domain architecture analysis of VM proteins. Previous work identified a group I pathogen-specific family of paralogous *Leptospira* proteins uninformatively classified as PF07598 (DUF1561) that are expanded (≥12 copies/genome) in highly pathogenic members of the genus, e.g., *L. interrogans* serovar Lai, some of which including serovars Copenhageni and Canicola are cosmopolitan and of particular public health importance. The PF07598 gene family members were not associated with discernable pathogenicity islands, IS elements, nor virulence gene-related operons (12). Previous studies demonstrated that select paralogs were highly upregulated in vivo (14, 18) during mammalian infection and that some were necessary for virulence (14, 19, 20). Serovar Lai encodes 12 paralogs, whereas serovars Copenhageni and Manilae each contain 13 paralogs (Table 1, gene IDs/locus tags and corresponding Uniprot IDs of all PF07598 paralogs found in serovars Lai, Copenhageni and Manilae; those for which knockout mutants are available and have been implicated in virulence are indicated). Both LA3490 (Q8F0K3) and LA0620 (Q8F8D7) are present and highly conserved among all three serovars, with average amino acid

identities exceeding 99% (Table 2, and S1 Appendix 1 – 3). Serovars Copenhageni and Manilae, contain an additional ortholog, LIC_10639 (Q72UL8) and LMANV2_170032 (A0A2H1XAY7), respectively, sharing 94% amino acid identity that is absent from serovar Lai.

Apart from group I pathogenic *Leptospira,* PF07598 orthologs are found in a number of facultative intracellular bacterial genera including a large family in *Bartonella* (21, 22), and single copies in Campylobacterales (*Campylobacter* spp., *Helicobacter* spp.), *Piscirickettsiaceae*, Actinoplanes and some Vibrionaceae (12). Unlike highly pathogenic group I *Leptospira* (*L. interrogans*, *L. kirschneri* and *L. noguchii*) and *B. bacilliformis* and *B. australis* that contain 12 or more paralogs per genome, these other genomes encode only single copy homologs with only a few non-*Leptospira* genomes encoding multiple (as many as 4) additional paralogs. Multiple sequence alignment via MAFFT version 7 and protein-disordered structural analysis in Jalview v2.10.5 (S1 Fig) demonstrated that serovars Lai, Copenhageni, Manilae, Canicola, Hardjo and Pomona encode 10 – 12 long, multidomain paralogs (Fig 1A) with domain organization similar to but in reverse orientation of castor bean-produced ricin toxin (23), and distinct from most other bacteria-secreted exotoxins (24-28) that are usually encoded by two or more genes and assembled into multimeric protein complexes (26). All six serovars also contain a shortened PF07598 paralog containing a signal peptide but lacking the N-terminally located ricin B-like binding domain (Fig 1A and below).

Leptospiral ricin B-like domains have carbohydrate binding properties similar to that of ricin B chain. Phyre2 searching (http://www.sbg.bio.ic.ac.uk/phyre2) (15) identified a ricin B-like β-trefoil domain in the amino-terminal region of leptospiral VM proteins leading us to hypothesize that, like ricin B, and other ricin B-domain containing bacterial toxins, e.g., *Vibrio cholerae*

126 cytolysin, VCC (29), VM proteins ought to bind to host cell-surface glycoconjugates. We focused
127 here on Q8F0K3 (LA3490) because our previous data indicated that it is implicated in virulence
128 and is highly up-regulated in vivo (14). Recombinant Q8F0K3 (rLA3490) was expressed in *E. coli*
129 as an N-terminal fusion with thioredoxin and C-terminal fusion with mCherry and a His_6 tag to
130 facilitate folding and affinity purification and visualization of the protein using fluorescence
131 microscopy, respectively (Fig 1B). Because native ricin B binds to terminal galactosyl residues of
132 glycoconjugates (30), we used asialofetuin, a terminal galactosyl-containing glycoprotein used for
133 assaying the presence of ricin holotoxin (16, 17, 31), to determine whether rLA3490 would have
134 similar carbohydrate binding specificity. Soluble recombinant proteins, both full-length and
135 truncated, t3490 (i.e. partial ricin B domain, lacking the middle and C-terminal domains (putative
136 translocation and enzymatic)) (Fig 1B), were purified by nickel affinity chromatography, verified
137 by Western immunoblot, and determined to have low levels of endotoxin contamination using a
138 Limulus Amebocyte Lysate (LAL) assay (Fig 2). Binding and ricin B competition assays
139 confirmed that both rLA3490 and t3490 bound to asialofetuin, that binding was mediated by the
140 N-terminal carbohydrate binding domains (CBDs) and that these shared ligand specificity with
141 ricin B (Fig 3).
142
143 ***Full-length, rLA3490, but not t3490, causes cytopathic effects on HeLa cells.*** Some bacterial
144 cytotoxins such as those of *Bordetella pertussis, Bacillus anthracis, Pseudomonas aeruginosa,*
145 *Yersinia pestis*, *Vibrio cholerae* and *Salmonella typhi,* bind to cell surfaces, become internalized
146 and then exert their effects on one or more intracellular targets (28, 29, 32). Having established
147 that VM proteins contain *bona fide* N-terminal ricin B-like domains, we tested the hypothesis that
148 full-length VM proteins were indeed cytotoxins. Cytopathic effect including cell rounding and

149 blebbing (Fig 4A, and S1 + S2 Video), release of lactate dehydrogenase (Fig 4B), and cell death
150 (Fig 5A) and detachment (Fig 5B), occurred in HeLa cells treated with rLA3490. Such changes
151 were not observed with t3490, bovine serum albumin (BSA) or in untreated HeLa cells. Upon
152 exposure to rLA3490, HeLa cell adhesion was reduced significantly compared to controls (40%
153 vs >80%) (Fig 5B).

154 To further corroborate these findings, live-cell experiments using a transposon mutant of
155 serovar Manilae, M1439, containing a disrupted LA3490 ortholog (LMANV2_1700091, Table 1),
156 which had no cytopathic effect on HeLa cells, and an isogenic wildtype strain that had a
157 pronounced effect (Fig 6). To induce expression of LMANV2_1700091, *Leptospira* cells were
158 grown in liquid EMJH in the presence of 120mM NaCl plus 10% rat serum, conditions previously
159 shown to mimic the host environment (13, 33). Such conditioned *Leptospira* were used to infect
160 HeLa cell monolayers at a Multiplicity Of Infection (MOI) of 100:1. Whereas wildtype *L.*
161 *interrogans* serovar Manilae produced cytopathic effect within 2 h, neither M1439 nor the 'mild'
162 pathogen, *L. licerasiae* serovar Varillal, which lacks the PF07598 gene family entirely (12), had
163 any noticeable cytopathic effect, even 4 h post-infection (Fig 6), confirming that LA3490 and its
164 orthologs (e.g., LMANV2_1700091) have potent cytotoxic activity.

165

166 ***Full-length VM protein LA3490 is internalized by HeLa cells and is translocated to the nucleus.***
167 To test whether rLA3490 (and VM proteins in general) are internalized by HeLa cells, rLA3490-
168 and t3490-mCherry fusion proteins were visualized by super-resolution confocal microscopy
169 (Leica SP8 Gated STED 3X). Like t3490, rLA3490 bound to the cell surface, but the full length
170 protein was internalized and translocated to the nucleus. Maximum binding occurred 30 – 60

171 minutes post-exposure, with internalization, translocation and nuclear degradation evident from
172 30 min onwards; t3490 bound to the surface of HeLa cells but was not internalized (Fig 7).
173
174 ***Full-length VM protein rLA3490 induces actin depolymerization in HeLa cells.*** Internalization
175 of rLA3490 induced depolymerization of actin filaments producing cell rounding from 1 h
176 onwards after treatment (Fig 8A). The morphology of HeLa cells treated with t3490 (Fig 8B) or
177 BSA (Fig 8C), and untreated cells (Fig 8D) remained unaltered. The mechanism(s) by which
178 leptospiral VM proteins, such as LA3490, perturb actin polymerization merits further
179 investigation.
180
181 ***Distribution of VM paralogs among medically important* Leptospira *serovars, as potential***
182 ***prognostic biomarkers and implications for biotherapeutics.*** Based on publicly accessible
183 sequence data, it is clear that VM proteins have an extremely limited taxonomic distribution.
184 Among the organisms known to possess VM proteins, three species of *Leptospira* (*interrogans*,
185 *kirschneri* and *noguchii*), which comprise the most highly pathogenic *Leptospira*, and two species
186 of *Bartonella* (*bacilliformis* and *australis*) are exceptional in that their genomes contain 12 or more
187 distinct VM paralogs, whereas most other species including other, less virulent, group I pathogenic
188 *Leptospira* encode at most 5 paralogs. Previous comparative whole genome analysis of all (at the
189 time) recognized pathogenic *Leptospira* species hinted at a complex series of gene
190 duplications/deletions underpinning the uneven the distribution of VM proteins amongst
191 *Leptospira*. To further explore this phenomenon with an eye towards biomarker discovery and the
192 development of novel therapeutics, we performed a more focused analysis incorporating the
193 improved understanding of VM protein domain organization (targeting vs enzymatic) uncovered

194 here. Manually curated multiple sequence alignments (S1 Fig) were used to produce detailed
195 pairwise distance matrices of full-length proteins (S1 Appendix 1), and isolated lectin (S1
196 Appendix 2) and toxin domains (S1 Appendix 3) from six public-health important *L. interrogans*
197 serovars Lai (field mouse reservoir, and reference genome), Copenhageni (rat-borne), Canicola
198 (dogs), Hardjo (cattle), Manilae (rat-borne) and Pomona (broad host range including pigs) that
199 allow us to draw important conclusions. First, as might be expected, the N-terminally located
200 'targeting' lectin domains are on average more conserved (78% amino acid identity, amino acid
201 identity) than the C-terminal toxin domains (63% amino acid identity), consistent with our belief
202 that VM proteins are essentially lectin cytotoxins. Second, the range of targeting and toxin
203 functionalities varies amongst serovars, with both serovar-related duplications of certain lectin
204 domains and lectin domain-toxin domain combinations. For example, both the N- and C-terminal
205 domains of LA3490 are present and highly conserved (98.7% and 98.6% amino acid identity,
206 respectively) in all six serovars analyzed: Lai, Copenhageni, Canicola, Hardjo, Manilae and
207 Pomona. Whereas the full-length Lai and Copenhageni VM proteins are highly conserved between
208 each other in both lectin (99.6% amino acid identity) and toxin (99.7%) domains, in serovar
209 Canicola, for example, the LA3490 toxin domain (97.6% amino acid identity) is linked to a
210 different lectin domain shared with Q72UL8 (LIC_RS03300) (97.8% amino acid identity), which
211 itself occurrs in tandem with a distinct toxin domain (61.6% amino acid identity). In some paralogs,
212 e.g., Q72U83 and Q72NP1, the lectin domains are 100% conserved, but linked to distinct toxin
213 domains (70.7% amino acid identity), suggesting that apart from amino acid sequence variation in
214 either domain, domain shuffling to produce varied lectin and toxin domain combinations could
215 also contribute to the diversity of *Leptospira* VM proteins.

Based on the dramatically differing response of rLA3490- and rLA0620-treated HeLa cell monolayers, the observed sequence variation in the toxin domains could impact potency and/or mechanisms of toxicity. It is also evident that some serovars, e.g., Lai and Hardjo, and Canicola and Pomona have nearly perfect (>99% amino acid identity) conservation of their full-complement of lectin domains and may have similar cellular targets.

Discussion

Here we demonstrate that *Leptospira* Virulence Modifying (VM) proteins (12, 14) are *bona fide* R-type lectin domain-containing cytotoxins, virtually unique to pathogenic *Leptospira*, some of which rapidly kill mammalian cells after first binding to the cell surface, internalization and nuclear translocation. VM proteins produce cytopathic effect including cell rounding, cell membrane blebbing, pedestal formation, actin depolymerization, nuclear fragmentation and ultimately cell lysis and death. Most contain an N-terminal fragment containing an empirically verified carbohydrate binding domain (CBD) sharing binding specificity with ricin B chain for terminal galactosyl residues of glycoconjugates that likely mediates cell binding/targeting and internalization, and a more variable C-terminal domain (CTD) responsible for intracellular trafficking and cytotoxicity. The high amino acid identity of the N-terminally located ricin B-like domain enables grouping of *L. interrogans* serovars into host cell tropic or virulence groups based on pairwise comparisons of the full complement of N-terminal CBDs or C-terminal CTDs, respectively, based on their respective VM paralogs. The finding that certain VM protein homologs induce cytopathic effect is the first definitive evidence that certain serovars are intrinsically more virulent than others and therefore of heightened clinical and public health significance.

Like ricin, for which toxicity and pathology are clearly linked and route dependent (inhalation leading to severe respiratory compromise being most lethal), site-specific expression of select VM family members could be a parsimonious explanation of the famously poorly understood 'protean' manifestations of severe leptospirosis. Indeed, efforts to understand the molecular and cellular pathogenesis of leptospirosis remains in its infancy, and approaches to prevent leptospirosis or ameliorate its pathogenesis are predicated on mechanistic understandings of the biology of *Leptospira*-host interactions. For example, pulmonary hemorrhage and refractory shock are particularly important clinical manifestation of leptospirosis (34-41). Indirect evidence—that these serious manifestations are ameliorated by hemodialysis/hemofiltration (42, 43)—suggests that there may be circulating soluble toxin(s) in leptospirosis. Histopathological analysis of lung tissues in severe pulmonary leptospirosis syndrome do not find intact *Leptospira* (44), but rather damage to alveolar epithelial and activation of endothelial cells, which might explain deposition of immunoglobulin and complement as secondary events (45-47). The data we present here build on. our previously published observations (12-14) that showed *Leptospira* VM proteins to be major virulence factors, potentially involved in the molecular and cellular pathogenesis of leptospirosis. And crucially, new monoclonal antibody based 'biotherapeutics' targeting these seemingly potent *Leptospira* R-type cytotoxins could revolutionize patient care and could ameliorate severe manifestations of leptospirosis.

Extensive studies using transposon mutants indicate have shown that multiple distinct VM proteins, including LA0589, contribute to lethal disease in an experimental hamster model (20, 37). The present work is consistent with previous findings that LA3490 is among the most highly upregulated PF07598 family members *in vivo* (14). Phyre2-based *in silico* analysis indicated that VM proteins contain ricin B domains (R-type lectins), which was confirmed experimentally using

recombinant full-length VM protein (rLA3490) and N-terminal fragments containing isolated ricin B domains (t3490, t0620). R-type lectins belong to a superfamily of proteins containing a CBD named for and structurally similar to ricin B chain and are found in plants, animals, and bacteria (30). Ricin and its B chain (and other R-type lectins) bind to terminal galactoses or other related glycans of a diverse range of host cell surface glycoconjugates, which facilitates translocation and internalization of the ricin A chain into target cells, resulting in cell death via inhibition of protein synthesis (48-51). Likewise, most potent bacterial toxins such as Shiga, diphtheria and pertussis toxins mediate cell death either by ADP-ribosylation of 28S rRNA or by inactivation of elongation factor 2 (52-55). However, the less well-studied genotoxins, e.g., cytolethal distending toxins (CDTs), are endonucleases that exert their toxic activity following nuclear translocation, similar to LA3490.

While we demonstrated that ricin B domains of distinct VM proteins (LA3490 and LA0620) bound to immobilized asialofetuin (16, 56, 57), native target ligands and cellular targets are yet to be defined. Second, differences in cytopathic potential among VM proteins and molecular pathways by which these proteins exert their biological effects remain to be explored, though these initial experiments clearly indicate that toxicity is mediated by the CTD and is likely to differ among various VM family members because of substantial amino acid sequence variation in the C-terminal half of the molecule. Third, while sequence variation and domain shuffling account for the VM protein diversity, we do not yet understand the reasons for the expansion of PF07598 paralogs in *L. interrogans, L. kirschneri* and *L. noguchii* (14) compared to other pathogenic *Leptospira* species (12, 14), the uneven distribution of VM paralogs, which are clearly non-redundant (12), among medically-important serovars would imply that necessary targeting and toxin functionality are serovar-dependent with host adaptation a potential eco-evolutionary driver.

Materials and Methods

Bacterial strains. *Leptospira* were maintained at 30°C in semi-solid **E**llinghausen, **M**cCullough, **J**ohnson and **H**arris medium (EMJH, BD Biosciences, USA) (58). Isogenic, wild type *L. interrogans* serovar Manilae strain L459 (National Veterinary Services Laboratory, Ames, IA, USA), mutant M1439 (transposon mutant LMANV2_170091) (20) and *L. licerasiae* VAR010 (isolated from mild leptospirosis case in Peru) were cultured in liquid EMJH medium to a cell density of ~2 x 10^8 cells/mL supplemented with 120 mM NaCl and 10% rat serum (Rockland Immunochemicals, USA) to simulate the in vivo host environment and to induce virulence gene expression (59). *Leptospira* cells were harvested by centrifugation at 18,514 *g* for 20 min at 4°C (Eppendorf, USA), washed twice with cold 1X PBS, pH 7.4 (AmericanBio, USA), and then counted by dark-field microscopy via a Petroff-Hausser counting chamber (Fisher Scientific, USA).

Mammalian cell culture. HeLa cells were obtained from the **A**merican **T**ype **C**ulture **C**ollection (ATCC, USA) and maintained in **D**ulbecco's **M**odified **E**agle **M**edium (DMEM; Sigma-Aldrich, USA), supplemented with 10% fetal bovine serum and 1% antibiotic-antimycotic solution (penicillin, 100 units/mL; streptomycin, 100 μg/mL and amphotericin, 25 μg/mL; Invitrogen, USA) at 37°C in a humidified atmosphere containing 5% CO_2. Antibiotic-containing medium was replaced with fresh, antibiotic-free medium prior to experimental infection with *Leptospira*, which were done at a MOI of 100:1 for 4 h (60).

In silico analysis. To improve functional classification of PF07598, nucleotide sequences of LA3490 and LA0620 were uploaded to the online Phyre2 server

(http://www.sbg.bio.ic.ac.uk/phyre2) (15), which utilizes structural information to detect remote homologs. In addition, coding sequences of all full-length (excluding pseudogenes) PF07598 gene family members in *L. interrogans* serovars Lai strain 56601^{T} [12 paralogs], Cophenhageni L1-130 [13], Canicola [13], Hardjo subtype prajitno Norma [12], Manilae strain L495 [13], Pomona [12], and *L. kirschneri* Pomona [10] were downloaded from Uniprot (http://www.uniprot.com) and aligned using the MAFFT v7 ***einsi*** algorithm with default parameters (http://mafft.cbrc.jp/alignment/software). Poorly aligned regions were refined manually in Jalview v2.10.5, which was also used to predict secondary structure (JPred with default parameters (http://www.compbio.dundee.ac.uk/jpred/jalviewWS/service/JPred)), and to identify globular domains (GlobPlot with default parameters (http://globplot.embl.de)).

Plasmid constructs and cloning. The gene sequences of LA3490 (Gene Bank Accession number; NP_713670.1, 1920 bp) and LA0620 (NP_710801.1, 1914 bp) were retrieved from NCBI (https://www.ncbi.nlm.nih.gov). Sequences of full-length LA3490 without signal peptide (57 bp – 1920 bp) and N-terminal ricin domain of LA3490 (123 bp – 552 bp) were codon-optimized and fused with full-length mCherry (AST15061.1) as a fluorescent tag (708 bp) along with a glycine-serine hinge (Gly4S) and flanking N- and C-terminally located enterokinase recognition sites (Fig 1B). Synthetic genes were cloned into pET32b (+) (Gene Universal Inc., USA), and verified by sequencing.

Recombinant protein expression and purification. Because PF07598 gene family members are cysteine-rich, recombinant proteins were expressed in SHuffle®T7 competent *E. coli* cells (New England Biolabs, USA), due to their capacity to promote disulfide bonds in the cytoplasm ensuring

proper protein folding. Transformants were sub-cultured into Luria-Bertani (LB) medium containing 100 μg/mL ampicillin. When cultures had reached an OD of 0.6, expression was induced at 16°C and 250 rpm for 24 h via addition of 1 mM isopropylthio-β-D-galactoside (IPTG; Sigma-Aldrich, USA). Following induction, cells were pelleted then lysed in CelLytic™ B (Cell Lysis Reagent; Sigma-Aldrich, USA) containing 50 units benzonase (Sigma-Aldrich, USA), 0.2 μg/mL lysozyme, non-EDTA protease inhibitor (Roche, USA) and 100 mM PMSF (Sigma-Aldrich, USA) for 1 h at 37°C. Lysates were then centrifuged at 4°C and 18,514 *g* for 10 min, supernatants and pellets were separated, and protein concentration determined by BCA (Pierce™ BCA Protein Assay Kit, Thermo Scientific, USA). Proteins were analyzed by 4-12% bis-tris sodium dodecyl sulfate-polyacrylamide gel electrophoresis (SDS-PAGE). Purification was done using 5 mL pre-packed Ni-sepharose AKTA Hi-TRAP column (GE Healthcare, USA) equilibrated (100 mM NaH_2PO_4, 10 mM Tris-HCl, 25 mM imidazole, pH 8.0). Bound protein was eluted in buffer containing 500 mM imidazole, pH 8.0. Pooled eluates were concentrated using a 30 kDa amicon ultra-centrifugation tube (Merck Millipore, Germany) and washed two to three times with 1X PBS pH 7.4 at 4°C. Purified soluble recombinant proteins were tested for bacterial endotoxins using the **L**imulus **A**mebocyte **L**ysate (LAL) assay kit (Invitrogen, USA).

SDS-PAGE and Western immunoblot analysis. SDS-PAGE was performed according to the method of Laemmli (61). Proteins were stained with Coomassie Brilliant Blue R-250. For Western immunoblot analysis, proteins were transferred onto a nitrocellulose membrane. The membrane was blocked with 5% nonfat dry milk in 1X TBST (TBS + 1% Tween 20) buffer (AmericanBio, USA) for 2 h, and then probed with either mouse anti-His monoclonal antibody (1:2,000 dilution; Santa Cruz Biotechnology, USA) or mouse anti-LA3490 polyclonal antibodies and mouse anti-

353 LA0620 polyclonal antibodies (1:1,000 dilution), respectively. After washing with TBST, the blot
354 was incubated for 2½ h with alkaline phosphatase-conjugated goat anti-mouse IgG (H+L) as the
355 secondary antibody at dilution of 1:5000 dilution (KPL, USA). The blot was developed with ready-
356 to-use 5-bromo-4-chloro-3-indolyl phosphate and nitroblue tetrazolium solution (BCIP/NBT;
357 KPL, USA).
358
359 ***Asialofetuin binding and ricin B chain competitive binding assay***. Binding assays were done
360 using Immulon® 2HB flat-bottom microtiter plates (Thermo Fisher Scientific, USA). Plates were
361 coated with asialofetuin (250 ng/100 μL in carbonate-bicarbonate buffer, pH 9.4), incubated at
362 4°C for overnight, and then blocked with 5% non-fat skimmed milk in 1X TBST for 2 h at 37°C.
363 After blocking, rLA3490 and t3490 were added separately at a concentration of 50 nM (in 1X
364 TBST). Plates were incubated for 2 h; and washed three times with TBST prior to incubation for
365 1 h with anti-LA3490 polyclonal antibodies (1:1000 in TBST). Bound rLA3490/t3490 was
366 quantified as follows: plates were incubated with goat anti-mouse IgG (1:5000; KPL, USA) for 1
367 h, washed thrice with TBST and developed with p-Nitrophenyl phosphate (1-Step™ PNPP
368 Substrate Solution; KPL, USA). The reaction was stopped with 2 M NaOH, and absorbance was
369 read at 405nm on a SpectraMax® M2e Microplate Reader with preinstalled SoftMax® Pro 5.2
370 (Molecular Devices, USA).
371 For competitive binding assays, plates were pre-incubated with either 25 nM or 50 nM
372 recombinant ricin B chain (Vector Laboratories, USA) for 2 h before addition of 50 nM of
373 rLA3490 or t3490 and a final 2 h incubation. Bound rLA3490/t3490 was quantified as described
374 in the preceding paragraph.
375

376 ***rLA3490-mediated HeLa cell cytotoxicity***. HeLa cells (35,000 cells/200 μL) were seeded in 8 well
377 chamber slides (LabTek, USA) and incubated at 37°C in a humidified atmosphere containing 5%
378 CO_2 for 24 h. Cells were treated with 5 μg/mL of rLA3490 or t3490 for up to 4 h; BSA (5 μg/mL)
379 and untreated HeLa cells served as controls. Images were captured at 10X magnification using a
380 Leica DMi8 inverted microscope (Leica Microsystems, Germany). Adherent cells, before and after
381 4 h exposure to either rLA3490 or t3490, were counted using Leica Application Suite X (Leica
382 Microsystems, Germany).
383
384 ***Live/dead and F-actin staining, and LDH assay***. HeLa cells were treated with 5 μg/mL of
385 rLA3490 or t3490 for 4 h. The monolayer was washed twice with 1X PBS, pH 7.4. Two hundred
386 microliters of 2 μM calcein AM/4 μM ethidium homodimer-1 in PBS (Live/Dead® Viability Kit,
387 Invitrogen, USA) were added to the wells and plates incubated for 30 min in the dark. Monolayers
388 were washed with PBS pH 7.4 to mitigate non-specific, background fluorescence. BSA and
389 untreated HeLa cells were used as controls. Images were taken using a Leica DMi8 microscope at
390 10x magnification with appropriate excitation and emission filters for green (live cell) and for red
391 (dead) fluorescence. In addition, cell damage was quantified by assaying the release of lactate
392 dehydrogenase (CyQUANT™ LDH Cytotoxicity Assay, Invitrogen, USA).
393 For F-actin staining, cell monolayers were exposed for up to 1 h, washed twice with PBS,
394 pH 7.4, and then fixed with 4% paraformaldehyde (Sigma-Aldrich, USA) for 30 minutes at room
395 temperature. Following aspiration of the fixative, monolayers were washed twice with PBS, then
396 0.1% Triton X-100 in PBS was added to each well for 5 minutes prior to repeat washes with PBS.
397 Monolayers were incubated with phalloidin Alexa_488nm conjugate (Invitrogen, USA) at room
398 temperature for 30 minutes in the dark per manufacturer's directions. Nuclei were stained with 0.1

399 μg/mL of ProLong™ Gold Antifade Mountant with DAPI (Invitrogen, USA) for 10 minutes. All
400 images were taken using a Leica DMi8 microscope with appropriate filters (Alexa_488nm (green),
401 DAPI (blue)) at 40x magnification.
402
403 ***Internalization of rLA3490 by HeLa cells***. HeLa cells were seeded in 8 well chamber slides
404 (LabTek, USA) and incubated as described above. Monolayers were treated with 5 μg/mL of
405 rLA3490 or t3490 for up to 60 minutes, washed twice with PBS, and then stained with CellMask™
406 Green Plasma Membrane Stain (Invitrogen, USA) per manufacturer's directions. Images were
407 taken using a Leica SP8 Gated STED 3X super resolution confocal microscope (Leica
408 Microsystems, Germany) at 100x with appropriate filters.
409
410 ***Statistical analysis***. All experiments were performed in triplicate. Results were expressed as mean
411 and standard deviation and non-parametric *t*-test was used to assess statistical significance in Graph
412 Prism 8.
413
414 **Acknowledgments**
415 The work reported benefitted from the use of a (knockout) mutant strain of *L. interrog*ans serovar
416 Manilae containing a transposon inactivated LA3490 ortholog that was a kind gift of Ben Adler,
417 Gerald Murray and Mathieu Picardeau.
418
419 **Conflict of interest**
420 The authors declare that there is no conflict of interest regarding the publication of this paper.
421

References

1. Costa F, Hagan JE, Calcagno J, Kane M, Torgerson P, Martinez-Silveira MS, et al. Global Morbidity and Mortality of Leptospirosis: A Systematic Review. PLoS Negl Trop Dis. 2015;9(9):e0003898.
2. Rudd KE, Johnson SC, Agesa KM, Shackelford KA, Tsoi D, Kievlan DR, et al. Global, regional, and national sepsis incidence and mortality, 1990-2017: analysis for the Global Burden of Disease Study. Lancet. 2020;395(10219):200-11.
3. Torgerson PR, Hagan JE, Costa F, Calcagno J, Kane M, Martinez-Silveira MS, et al. Global Burden of Leptospirosis: Estimated in Terms of Disability Adjusted Life Years. PLoS Negl Trop Dis. 2015;9(10):e0004122.
4. Jimenez JIS, Marroquin JLH, Richards GA, Amin P. Leptospirosis: Report from the task force on tropical diseases by the World Federation of Societies of Intensive and Critical Care Medicine. Journal of critical care. 2018;43:361-5.
5. Ellis WA. Animal leptospirosis. Curr Top Microbiol Immunol. 2015;387:99-137.
6. Ko AI, Goarant C, Picardeau M. Leptospira: the dawn of the molecular genetics era for an emerging zoonotic pathogen. Nat Rev Microbiol. 2009;7(10):736-47.
7. Adler B, de la Pena Moctezuma A. Leptospira and leptospirosis. Vet Microbiol. 2010;140(3-4):287-96.
8. Haake DA, Levett PN. Leptospirosis in humans. Curr Top Microbiol Immunol. 2015;387:65-97.
9. Evangelista KV, Coburn J. Leptospira as an emerging pathogen: a review of its biology, pathogenesis and host immune responses. Future Microbiol. 2010;5(9):1413-25.

444 10. Chin VK, Basir R, Nordin SA, Abdullah M, Sekawi Z. Pathology and Host Immune Evasion
445 During Human Leptospirosis: a Review. Int Microbiol. 2019.
446 11. Picardeau M. Virulence of the zoonotic agent of leptospirosis: still terra incognita? Nat Rev
447 Microbiol. 2017;15(5):297-307.
448 12. Fouts DE, Matthias MA, Adhikarla H, Adler B, Amorim-Santos L, Berg DE, et al. What
449 Makes a Bacterial Species Pathogenic?:Comparative Genomic Analysis of the Genus
450 Leptospira. PLoS Negl Trop Dis. 2016;10(2):e0004403.
451 13. Matsunaga J, Lo M, Bulach DM, Zuerner RL, Adler B, Haake DA. Response of Leptospira
452 interrogans to physiologic osmolarity: relevance in signaling the environment-to-host
453 transition. Infect Immun. 2007;75(6):2864-74.
454 14. Lehmann JS, Fouts DE, Haft DH, Cannella AP, Ricaldi JN, Brinkac L, et al. Pathogenomic
455 inference of virulence-associated genes in Leptospira interrogans. PLoS Negl Trop Dis.
456 2013;7(10):e2468.
457 15. Kelley LA, Mezulis S, Yates CM, Wass MN, Sternberg MJ. The Phyre2 web portal for protein
458 modeling, prediction and analysis. Nat Protoc. 2015;10(6):845-58.
459 16. Dawson RM, Paddle BM, Alderton MR. Characterization of the Asialofetuin microtitre plate-
460 binding assay for evaluating inhibitors of ricin lectin activity. J Appl Toxicol. 1999;19(5):307-
461 12.
462 17. Blome MC, Petro KA, Schengrund CL. Surface plasmon resonance analysis of ricin binding
463 to plasma membranes isolated from NIH 3T3 cells. Anal Biochem. 2010;396(2):212-6.
464 18. Xu Y, Zhu Y, Wang Y, Chang YF, Zhang Y, Jiang X, et al. Whole genome sequencing
465 revealed host adaptation-focused genomic plasticity of pathogenic Leptospira. Sci Rep.
466 2016;6:20020.

19. Marcsisin RA, Bartpho T, Bulach DM, Srikram A, Sermswan RW, Adler B, et al. Use of a high-throughput screen to identify Leptospira mutants unable to colonize the carrier host or cause disease in the acute model of infection. Journal of Medical Microbiology. 2013;62:1601-8.

20. Murray GL, Morel V, Cerqueira GM, Croda J, Srikram A, Henry R, et al. Genome-wide transposon mutagenesis in pathogenic Leptospira species. Infect Immun. 2009;77(2):810-6.

21. Mullins KE, Hang J, Jiang J, Leguia M, Kasper MR, Maguina C, et al. Molecular typing of "Candidatus Bartonella ancashi," a new human pathogen causing verruga peruana. J Clin Microbiol. 2013;51(11):3865-8.

22. Blazes DL, Mullins K, Smoak BL, Jiang J, Canal E, Solorzano N, et al. Novel Bartonella agent as cause of verruga peruana. Emerg Infect Dis. 2013;19(7):1111-4.

23. Olsnes S, Refsnes K, Pihl A. Mechanism of action of the toxic lectins abrin and ricin. Nature. 1974;249(458):627-31.

24. Bumba L, Masin J, Fiser R, Sebo P. Bordetella adenylate cyclase toxin mobilizes its beta2 integrin receptor into lipid rafts to accomplish translocation across target cell membrane in two steps. PLoS Pathog. 2010;6(5):e1000901.

25. Leppla SH. Anthrax toxin edema factor: a bacterial adenylate cyclase that increases cyclic AMP concentrations of eukaryotic cells. Proc Natl Acad Sci U S A. 1982;79(10):3162-6.

26. Rudkin JK, McLoughlin RM, Preston A, Massey RC. Bacterial toxins: Offensive, defensive, or something else altogether? PLoS Pathog. 2017;13(9):e1006452.

27. Spangler BD. Structure and function of cholera toxin and the related Escherichia coli heat-labile enterotoxin. Microbiol Rev. 1992;56(4):622-47.

28. Galan JE. Typhoid toxin provides a window into typhoid fever and the biology of Salmonella Typhi. Proc Natl Acad Sci U S A. 2016;113(23):6338-44.

29. Olson R, Gouaux E. Vibrio cholerae cytolysin is composed of an alpha-hemolysin-like core. Protein Sci. 2003;12(2):379-83.

30. Cummings RD, Schnaar RL. Chapter 31: R-Type Lectins. In: Varki A, Cummings RD, Esko JD, editors. Essentials of Glycobiology [Internet] 3rd edition. Cold Spring Harbor (NY): Cold Spring Harbor Laboratory Press; 2017.

31. Sehnke PC, Pedrosa L, Paul AL, Frankel AE, Ferl RJ. Expression of active, processed ricin in transgenic tobacco. J Biol Chem. 1994;269(36):22473-6.

32. Ahuja N, Kumar P, Bhatnagar R. The adenylate cyclase toxins. Crit Rev Microbiol. 2004;30(3):187-96.

33. Narayanavari SA, Lourdault K, Sritharan M, Haake DA, Matsunaga J. Role of sph2 Gene Regulation in Hemolytic and Sphingomyelinase Activities Produced by Leptospira interrogans. PLoS Negl Trop Dis. 2015;9(8):e0003952.

34. Sehgal SC, Murhekar MV, Sugunan AP. Outbreak of leptospirosis with pulmonary involvement in north Andaman. Indian J Med Res. 1995;102:9-12.

35. Gouveia EL, Metcalfe J, de Carvalho AL, Aires TS, Villasboas-Bisneto JC, Queirroz A, et al. Leptospirosis-associated severe pulmonary hemorrhagic syndrome, Salvador, Brazil. Emerg Infect Dis. 2008;14(3):505-8.

36. Helmerhorst HJ, van Tol EN, Tuinman PR, de Vries PJ, Hartskeerl RA, Grobusch MP, et al. Severe pulmonary manifestation of leptospirosis. Neth J Med. 2012;70(5):215-21.

37. Truong KN, Coburn J. The emergence of severe pulmonary hemorrhagic leptospirosis: questions to consider. Front Cell Infect Microbiol. 2011;1:24.

512 38. Ruwanpura R, Rathnaweera A, Hettiarachchi M, Dhahanayake K, Amararatne S. Severe
513 pulmonary leptospirois associated with high fatality rate: an autopsy series in galle, southern
514 sri lanka. Med J Malaysia. 2012;67(6):595-600.
515 39. Ko AI, Galvao Reis M, Dourado CMR, Johnson WD, Riley LW. Urban epidemic of severe
516 leptospirosis in Brazil. Lancet. 1999;354:820-5.
517 40. Segura E, Ganoza C, Campos K, Ricaldi JN, Torres S, Silva H, et al. Clinical spectrum of
518 pulmonary involvement in leptospirosis in an endemic region, with quantification of
519 leptospiral burden. Clin Infect Dis. 2005;40:343-51.
520 41. Marotto PC, Nascimento CM, Eluf-Neto J, Marotto MS, Andrade L, Sztajnbok J, et al. Acute
521 lung injury in leptospirosis: clinical and laboratory features, outcome, and factors associated
522 with mortality. Clin Infect Dis. 1999;29(6):1561-3.
523 42. Andrade L, Cleto S, Seguro AC. Door-to-dialysis time and daily hemodialysis in patients with
524 leptospirosis: impact on mortality. Clin J Am Soc Nephrol. 2007;2(4):739-44.
525 43. Cleto SA, Rodrigues CE, Malaque CM, Sztajnbok J, Seguro AC, Andrade L.
526 Hemodiafiltration Decreases Serum Levels of Inflammatory Mediators in Severe
527 Leptospirosis: A Prospective Study. PLoS One. 2016;11(8):e0160010.
528 44. Nicodemo AC, Duarte MIS, Alves VAF, Takakura CFH, Santos RTM, Nicodemo EL. Lung
529 lesions in human leptospirosis: Microscopic, Immunohistochemical, and ultrastructural
530 features related to thrombocytopenia. American Journal of Tropical Medicine and Hygiene.
531 1997;56(2):181-7.
532 45. Nally JE, Chantranuwat C, Wu XY, Fishbein MC, Pereira MM, Da Silva JJ, et al. Alveolar
533 septal deposition of immunoglobulin and complement parallels pulmonary hemorrhage in a
534 guinea pig model of severe pulmonary leptospirosis. Am J Pathol. 2004;164(3):1115-27.

535 46. Croda J, Neto AN, Brasil RA, Pagliari C, Nicodemo AC, Duarte MI. Leptospirosis pulmonary
536 haemorrhage syndrome is associated with linear deposition of immunoglobulin and
537 complement on the alveolar surface. Clin Microbiol Infect. 2010;16(6):593-9.
538 47. De Brito T, Aiello VD, da Silva LF, Goncalves da Silva AM, Ferreira da Silva WL, Castelli
539 JB, et al. Human hemorrhagic pulmonary leptospirosis: pathological findings and
540 pathophysiological correlations. PLoS One. 2013;8(8):e71743.
541 48. Sperti S, Montanaro L, Mattioli A, Stirpe F. Inhibition by ricin of protein synthesis in vitro:
542 60 S ribosomal subunit as the target of the toxin. Biochem J. 1973;136(3):813-5.
543 49. Montanaro L, Sperti S, Stirpe F. Inhibition by ricin of protein synthesis in vitro. Ribosomes
544 as the target of the toxin. Biochem J. 1973;136(3):677-83.
545 50. Lord MJ, Jolliffe NA, Marsden CJ, Pateman CS, Smith DC, Spooner RA, et al. Ricin.
546 Mechanisms of cytotoxicity. Toxicol Rev. 2003;22(1):53-64.
547 51. Sowa-Rogozinska N, Sominka H, Nowakowska-Golacka J, Sandvig K, Slominska-
548 Wojewodzka M. Intracellular Transport and Cytotoxicity of the Protein Toxin Ricin. Toxins
549 (Basel). 2019;11(6).
550 52. Cemal G. Design and construction of membrane-acting immunotoxins for intracellular and
551 secreted protein expression in Pichia pastoris. Thesis1999.
552 53. Brown JE, Ussery MA, Leppla SH, Rothman SW. Inhibition of protein synthesis by Shiga
553 toxin: activation of the toxin and inhibition of peptide elongation. FEBS Lett. 1980;117(1):84-
554 8.
555 54. Cherubin P, Quinones B, Teter K. Cellular recovery from exposure to sub-optimal
556 concentrations of AB toxins that inhibit protein synthesis. Sci Rep. 2018;8(1):2494.

557 55. Coutte L, Locht C. Investigating pertussis toxin and its impact on vaccination. Future
558 Microbiol. 2015;10(2):241-54.
559 56. Frankel AE, Burbage C, Fu T, Tagge E, Chandler J, Willingham MC. Ricin toxin contains at
560 least three galactose-binding sites located in B chain subdomains 1 alpha, 1 beta, and 2
561 gamma. Biochemistry. 1996;35(47):14749-56.
562 57. Wales R, Gorham HC, Hussain K, Roberts LM, Lord JM. Ricin B chain fragments expressed
563 in Escherichia coli are able to bind free galactose in contrast to the full length polypeptide.
564 Glycoconj J. 1994;11(4):274-81.
565 58. Ellinghausen HC, Jr., McCullough WG. Nutrition of Leptospira Pomona and Growth of 13
566 Other Serotypes: A Serum-Free Medium Employing Oleic Albumin Complex. Am J Vet Res.
567 1965;26:39-44.
568 59. Matsunaga J, Sanchez Y, Xu X, Haake DA. Osmolarity, a key environmental signal
569 controlling expression of leptospiral proteins LigA and LigB and the extracellular release of
570 LigA. Infect Immun. 2005;73(1):70-8.
571 60. Jin D, Ojcius DM, Sun D, Dong H, Luo Y, Mao Y, et al. Leptospira interrogans induces
572 apoptosis in macrophages via caspase-8- and caspase-3-dependent pathways. Infect Immun.
573 2009;77(2):799-809.
574 61. Laemmli UK. Cleavage of structural proteins during the assembly of the head of
575 bacteriophage T4. Nature. 1970;227(5259):680-5.
576

Table 1. PF07598 gene family members in select Group 1 pathogenic *Leptospira*

L. interrogans serovar Lai strain 56601			*L. interrogans* serovar Copenhageni strain 495			*L. interrogans* serovar Manilae strain 495		
Gene locus	**Reference / Protein ID**	**Amino acid**	**Gene locus**	**Reference / Protein ID**	**Amino acid**	**Gene locus**	**Reference / Protein ID**	**Amino acid**
LA_3388	Q8F0V3	631	LIC_10778	Q72U83	631	LMANV2_260038	A0A2H1XD57	631
LA_0835	Q8F7V7	631	LIC_12791	Q72NP1	631	LMANV2_240079	A0A2H1XD04	438
LA_0591#	Q8F8G6	313	LIC_12985#	Q72N53	313	LMANV2_70075#	A0A2H1XLT9	314
LA_0589(V)	Q8F8G8	632	LIC_12986	Q72N52	632	LMANV2_70078	A0A2H1XJZ3	549
LA_1402	Q8F6A7	641	LIC_12339	Q72PX8	663	LMANV2_210058	A0A2H1XCB0	640
LA_1400	Q8F6A9	573	LIC_12340	Q72PX7	627	LMANV2_210056	A0A2H1XC81	627
LA_3271	Q8F166	636	LIC_10870	Q72TZ4	636	LMANV2_80114	A0A2H1XKP0	638
LA_0934	Q8F7L0	638	LIC_12715	Q72NW3	638	LMANV2_320010	A0A2H1XE97	638
LA_0769	Q8F820	602	LIC_12844	Q72NJ0	639	LMANV2_240142	A0A2H1XCY6	639
LA_2628	Q8F2Y3	638	LIC_11358	Q72SM1	638	LMANV2_150103	A0A2H1XAR4	638
NA	-	-	LIC_10639	Q72UL8	640	LMANV2_170032	A0A2H1XAY7	638
LA_0620	Q8F8D7	637	LIC_12963	Q72N74	637	LMANV2_70050	A0A2H1XJU7	637
LA_3490	Q8F0K3	639	LIC_10695	Q72UG2	639	LMANV2_170091	A0A2H1XB88	637

NA Not applicable due to a missing ortholog

Signal peptide and complete C-terminal fragment but missing entire N-terminal ricin B chain-like binding domain

V Only mutant unable to infect hamster

582 **Table 2. Average amino acid identity of LA3490 found in important *L. interrogans* serovars (full-length, N-terminal**
583 **carbohydrate binding domain and C-terminal putative toxin domain shown).**
584

Serovars	Lai					
	UniProt Protein ID	LA_3490/Q8F0K3		Uniprot Protein ID	LA_0620/Q8F8D7	
Copenhageni	Q72UG2	99.7		Q72N74	99.7	
		99.6	99.7		99.6	99.7
Manilae	A0A2H1XB88	97.4		A0A2H1XJU7	98.5	
		98.7	98.4		97.8	98.9
Canicola	A0A1X8WIC7	99.7		A0A1R0JW34	97.6	
		97.8	99.7		97.8	97.3
Hardjo subtype *prajitno*	A0A0M4NB61	100		A0A0M3TMJ8	99.7	
		100	100		99.1	100
Pomona	A0A163QL98	93.5		A0A163P0K6	974	
		97.3	97.3		97.3	97.3
Amino acid identity		98.4			98.6	
		98.9	98.9		99.1	98.9

585

Full length
Putative N-terminal ricin B-chain domain
Putative C-terminal enzymatic domain

587 **Supporting Information**

588 **S1 Figure.** Amino acid multiple sequence alignment of all full length PF07598 paralogs present
589 in serovars Lai, Copenhageni, Canicola, Hardjo and Pomona.

590

591 **S1 Appendices (1-3)**. Pairwise distance matrices of full-length (S1 Appendix 1), N-terminal ricin
592 B chain-like carbohydrate binding domain (S1 Appendix 2) and C-terminal toxin domain (S1
593 Appendix 3). Pairwise distances of Lai, Copenhageni and Canicola have been conditionally
594 formatted, and all others de-emphasized for easier viewing. Cells colored shades of green indicate
595 low amino acid identity —darker shades = lowest; whereas those colored shades of blue indicate
596 higher amino acid identity —darker shades = highest. Orthologous pairs have been indicated.

597

598 **S1 Video. Time-lapse video showing cytopathic effect in rLA3490-treated HeLa cells as early**
599 **as 50 min post-exposure**. Time-lapse images (40 frames, 5 s intervals) of rLA3490-treated HeLa
600 cells, 0 to 4 h post-exposure showing noticeable cytopathic effect as early as 50 minutes post-
601 exposure. rLA3490 was added at a final concentration of 5 μg/mL. Images were captured using a
602 Leica DMi8 inverted microscope at 40x magnification. Scale bar 10 μm.

603

604 **S2 Video. Time-lapse video of untreated HeLa cells up to four hours post-exposure.** Time-
605 lapse images (40 frames, 5 s intervals) of untreated HeLa cells (control) 0 to 4 h post-exposure
606 showing no morphological changes. Images were captured using a Leica DMi8 inverted
607 microscope at 40x magnification. Scale bar 10 μm.

608

609 **S3 Video. Orthogonal projections of t3490-treated HeLa cells, 30 min post-exposure.** Top left
610 and bottom right panels show binding of mCherry-t3490 fusion protein (red) at HeLa cell surface
611 30 minutes post-exposure. Plasma membrane and nucleus stained with CellMask™ Green Plasma
612 Membrane Stain and ProLong™ Gold Antifade Mountant with DAPI (blue), respectively. Images
613 captured using a Leica SP8 Gated STED 3X super-resolution confocal microscope. Magnification
614 100x.
615
616 **S4 Video. Orthogonal projections of t3490-treated HeLa cells, 60 min post-exposure.** Top left
617 and bottom right panels show binding of mCherry-t3490 fusion at HeLa cell surface 60 minutes
618 post-exposure. Plasma membrane and nucleus stained with CellMask™ Green Plasma Membrane
619 Stain and ProLong™ Gold Antifade Mountant with DAPI, respectively. Images captured using a
620 Leica SP8 Gated STED 3X super-resolution confocal microscope. Magnification 100x.
621
622 **S5 Video. Z-stacks of t3490-treated HeLa cells, 30 min post-exposure.** Animation of 24 cross-
623 sectional images (total depth, 6.87 μm; separation, 298.5 nm), with binding of mCherry-t3490
624 fusion evident at HeLa cell surface. Cells were washed twice with PBS, and the plasma membrane
625 and nucleus stained with CellMask™ Green Plasma Membrane Stain and ProLong™ Gold
626 Antifade Mountant with DAPI, respectively. Images captured using a Leica SP8 Gated STED 3X
627 super-resolution confocal microscope. Magnification 100x.
628
629 **S6 Video. Z-stacks of t3490-treated HeLa cells, 60 min post-exposure.** Animation of 32 cross-
630 sectional images (total depth, 9.25 μm; separation, 298.5 nm), with binding of mCherry-t3490
631 fusion still evident on HeLa cell surface (i.e. no internalization). Cells were washed twice with

PBS, and plasma membrane and nucleus stained with CellMask™ Green Plasma Membrane Stain and ProLong™ Gold Antifade Mountant with DAPI, respectively. Images captured using a Leica SP8 Gated STED 3X super-resolution confocal microscope. Magnification 100x.

S7 Video. Orthogonal projections of HeLa cells treated with rLA3490, 30 min post-exposure. mCherryr-LA3490 fusion on the HeLa cell surface 30 minutes of post-exposure, with internalization evident (top left, runtime 3 s; and bottom right, runtime 10 s). Plasma membrane and nucleus were stained with CellMask™ Green Plasma Membrane Stain and ProLong™ Gold Antifade Mountant with DAPI, respectively. Images were captured using a Leica SP8 Gated STED 3X super-resolution confocal microscope. Magnification 100x.

S8 Video. Orthogonal projections of HeLa cells treated with rLA3490, 60 min post-exposure. Internalized mCherryr-LA3490 fusion evident in all four images. Plasma membrane and nucleus were stained with CellMask™ Green Plasma Membrane Stain and ProLong™ Gold Antifade Mountant with DAPI, respectively. Images were captured using a Leica SP8 Gated STED 3X super-resolution confocal microscope. Magnification 100x.

S9 Video. Z-stacks of HeLa cells treated with rLA3490, 30 min post-exposure. Animation of 35 cross-sectional images (total depth, 10.15 μm; separation, 298.5 nm) showing binding of mCherry-rLA3490 fusion to HeLa cell surface. Plasma membrane and nucleus were stained with CellMask™ Green Plasma Membrane Stain and ProLong™ Gold Antifade Mountant with DAPI, respectively. Images were captured using a Leica SP8 Gated STED 3X super-resolution confocal microscope. Magnification 100x.

656 **S10 Video. Z-stacks of HeLa cells treated with rLA3490, 60 min post-exposure.** Animation of
657 42 cross-sectional images (total depth, 12.24 μm; separation, 298.5 nm) showing cell membrane
658 binding and internalization of mCherry-rLA3490 fusion. Plasma membrane and nucleus stained
659 with CellMask™ Green Plasma Membrane Stain and ProLong™ Gold Antifade Mountant with
660 DAPI, respectively. Images captured using a Leica SP8 Gated STED 3X super-resolution confocal
661 microscope. Magnification 100x.
662
663 **Figure legends**
664 **Fig 1. Proposed domain organization of VM proteins, and strategy for cloning of full-length**
665 **and N-terminal ricin B domain of LA3490**. **(A)** Schematic illustration of VM protein domain
666 organization showing the presence of an N-terminal ricin B domain, hydrophobic patch (*)
667 presumed to mediate insertion into endosome membrane prior to the extrusion and release of C-
668 terminal toxin domain to the cytosol. **SS**; signal sequences identified by SignalP. All VM proteins
669 share the LA3490 (Q8F0K3; 639 aa) domain organization depicted, though all serovars also
670 contain a short VM protein variant, e.g., LA0591 (Q8F8G6; 313 aa) and LMANV2_240079
671 (A0A2H1XD04; 438 aa), containing a SS and complete enzymatic domain (with hydrophobic
672 patch) but lacking the entire N-terminal ricin B binding domain. For reference, the domain
673 organization of plant derived ricin (*Ricinus communis*; P02879, 565 aa), the secreted Community-
674 Acquired Respiratory Distress syndrome (CARDs) toxin of *Mycoplasma pneumoniae* (P75409,
675 591 aa) and *diphtheria toxin* (*Corynebacterium diphtheriae*; Q5PY51, 535 aa) have been included.
676 Unlike VM proteins, the domain order is reversed in these and other "protoxins" typically encoded
677 by a single polypeptide chain. CARDs and diphtheria toxin belong to the family of ADP-
678 ribosylating toxins; whereas, ricin inactivates the ribosome and inhibits protein synthesis. **(B)**

679 Schematic depicting the organization of the recombinant mCherry fusion proteins used in the
680 current study; **rLA3490** full-length, nucleotide positions 57 - 1920 (minus SS); and **t3490**, 213 -
681 552, also lacking SS. Recombinant fusions also include a glycine-serine (Gly4S) linker (for
682 flexibility), C-terminal His6 tag (purification), and two internal enterokinase recognition sites.
683
684 **Fig 2. Evaluation of the purity of recombinant t3490 and rLA3490 fusion proteins by**
685 **Western blot and Limulus Amebocyte Lysate assay.** (**A**+**B**) Western blot of purified soluble
686 recombinant proteins confirming the presence single bands of the expected size (**A**, t3490; and **B**,
687 rLA3490). Membranes were probed with anti-His6 and polyclonal anti-LA3490 antibodies (lane
688 two and three, respectively). **M** - molecular weight marker. (**C)** Limulus Amebocyte Lysate (LAL)
689 assay indicating no appreciable endotoxin contamination; *E. coli* LPS used as positive control.
690 Data were visualized in GraphPad Prism v8.
691
692 **Fig 3. Asialofetuin- and ricin B chain competitive-binding assay.** Asialofetuin binding assay
693 confirming that both truncated (**t3490** or **t0620**) and full-length (**rLA3490**) VM proteins bind
694 asialofetuin in the absence (0 nM) of commercially available ricin B chain; and that binding is
695 inhibited by increasing concentrations of ricin B chain (25 nM and 50 nM). Assays were performed
696 in microtiter plates using an ELISA format. Mouse polyclonal anti-LA3490 and anti-LA0620
697 antibodies (1:1000 dilution) were used as primary and anti-mouse IgG as secondary antibody (used
698 alone as a specificity control). Assays were run in triplicate and experiments repeated at least twice
699 to assess consistency. The mean absorbance (±SEM) were visualized in GraphPad Prism 8 (data
700 from a representative experiment shown).
701

Fig 4. HeLa cell morphology and integrity upon exposure to t3490 and rLA3490. **(A)** Phase contrast images showing alteration of HeLa cell morphology following 4 h exposure to 5 μg/mL of rLA3490, with cell lysis confirmed by the release of lactate dehydrogenase at 1-hour intervals up to 4 h post exposure **(B)**. No such alterations, nor release of LDH, were observed in BSA-treated (5 μg/mL) or untreated cells **(A, B)**. Images were captured at 10x magnification using a Leica DMi8 inverted microscope. Scale bar, 100 μm. Mean absorbance of samples run in triplicate (±SEM) were visualized in GraphPad Prism 8.

Fig 5. Integrity of HeLa cell monolayers following exposure to t3490 and rLA3490. (A) Live/dead staining of HeLa cell monolayers following 4-h exposure to 5 μg/mL t3490 (top left panel) and rLA3490 (bottom left), showing a dramatic decrease of adherent cells and concomitant accumulation of dead cells upon exposure to rLA3490, but not t3490- or BSA-treated or untreated monolayers. Images were captured at 10x magnification using a Leica DMi8 inverted microscope. Scale bar, 100 μm. **(B)** Cell adherence following 4-h exposure to t3490 and rLA3490. Relative to BSA treated and untreated controls, rLA3490, but not t3490, significantly reduced the proportion of adherent cells indicating that N-terminal fragment alone is unable to cause cell death **(A**, **B)**. The impact of the various treatments was evaluated via Z-test and considered significant when $\boldsymbol{p} < 0.05$, **ns** = non-significant.

Fig 6. Cytopathic effect of LA3490 knockout mutant strain of *L. interrogans* serovar Manilae and (isogenic) wildtype strain on HeLa cell monolayers. Phase contrast images of HeLa cell monolayers in co-culture with three *Leptospira* strains for up to four hours. Row **1**: transposon mutant, M1439, containing an inactivated LA3490 ortholog, LMANV2_1700091; row **2**: isogenic

725 wild type strain; row **3**: low-virulence Group II pathogen, *L. licerasiae* serovar Varillal; and row
726 **4**: uninfected HeLa cell monolayers (control). To induce expression of LMANV2_1700091,
727 *Leptospira* were grown in liquid EMJH supplemented with 120 mM NaCl and 10% rat serum,
728 mimicking the *in vivo* host environment, then used to infect HeLa cell monolayers at a multiplicity
729 of infection of 100:1. Infected monolayers were incubated for up to four hours, with images taken
730 at 1-h intervals for the duration at 10x magnification using a Leica DMi8 confocal microscope.
731 Scale bar, 100 μm.
732
733 **Fig 7. Intracellular trafficking and localization of rLA3490 in HeLa cells**. Confocal images
734 show that whereas both **mCherry-rLA3490** and **-t3490** fusion proteins bind to the cell surface (**A**
735 and **B**, respectively), only rLA3490 is internalized. Z-stack images showing **mCherry-rLA3490**
736 fusion was internalized from 30 min onwards, with nuclear translocation and chromosomal
737 degradation (evinced by patchy DAPI staining; **A**, panel four, lower right) evident within 60
738 minutes. Monolayers were exposed to 5 μg/mL recombinant fusion protein or BSA for 30 minutes
739 and 60 minutes (or were left untreated). Cells were washed, stained with CellMaskTM Green
740 Plasma Membrane Stain, and then mounted with ProLong™ Gold Antifade Mountant +DAPI.
741 Images were captured at 100x using appropriate filters (blue, DAPI; green, plasma membrane; and
742 red, mCherry fusions).
743
744 **Fig 8. Full-length LA3490 mediated depolymerization of F-actin of HeLa cells.** HeLa cell
745 monolayers were incubated with 5 µg/mL of each of rLA3490 **(A),** t3490 **(B)**, and BSA **(C)** up to
746 1 h. Monolayers were fixed with 4% paraformaldehyde for 30 minutes and then followed by
747 washes, 0.1% Triton X-100 in PBS was added to each well for 5 minutes. Monolayer was

748 incubated with phalloidin Alexa_488nm conjugate at room temperature for 30 minutes in dark,
749 washed twice and then mounted with ProLong™ Gold Antifade Mountant with DAPI for 10
750 minutes. Images were captured using a Leica DMi8 confocal microscope with appropriate filters
751 (Alexa_488nm (green), DAPI (blue)) at 40x magnification. Untreated HeLa cells served as
752 control **(D).** Scale bars 20 µm.
753
754
755
756

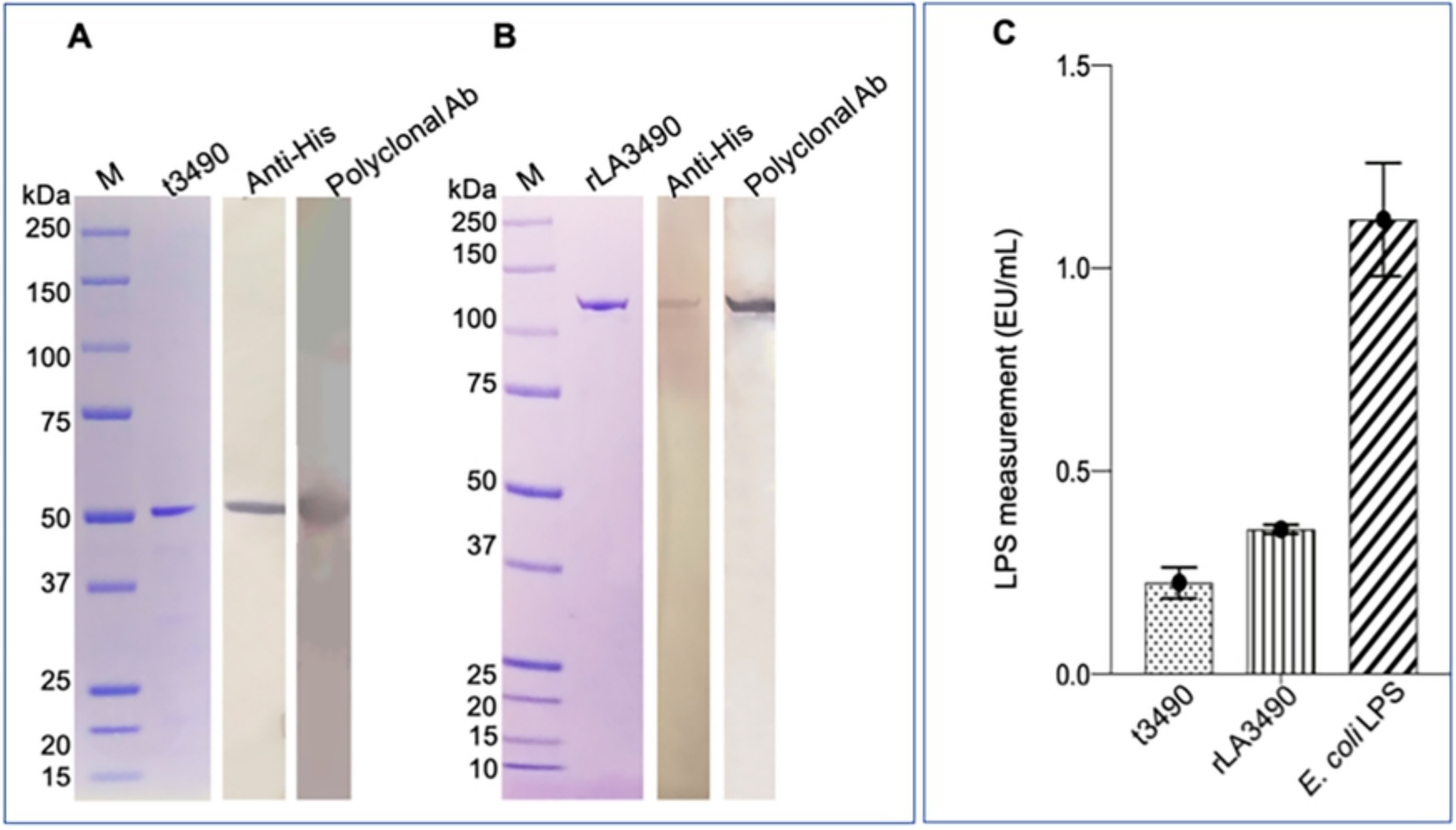
A
M
t3490
Anti-His
Polyclonal Ab
kDa
250
150
100
75
50
37
25
20
15
B
M
rLA3490
Anti-His
Polyclonal Ab
kDa
250
150
100
75
50
37
25
20
15
10
C
LPS measurement (EU/mL)
1.5
1.0
0.5
0.0
t3490
rLA3490
E. coli LPS

Figure 2

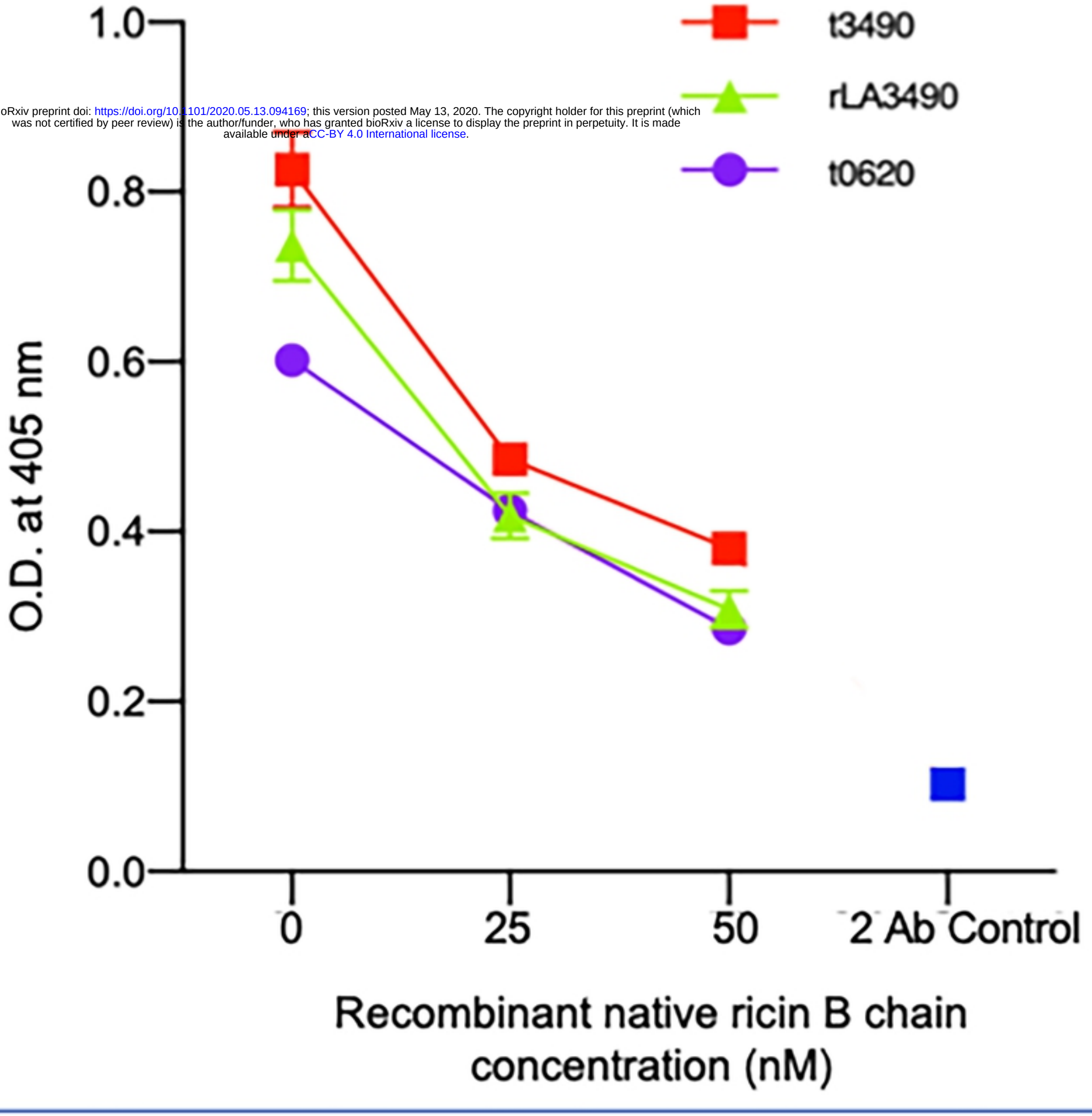

Figure 3

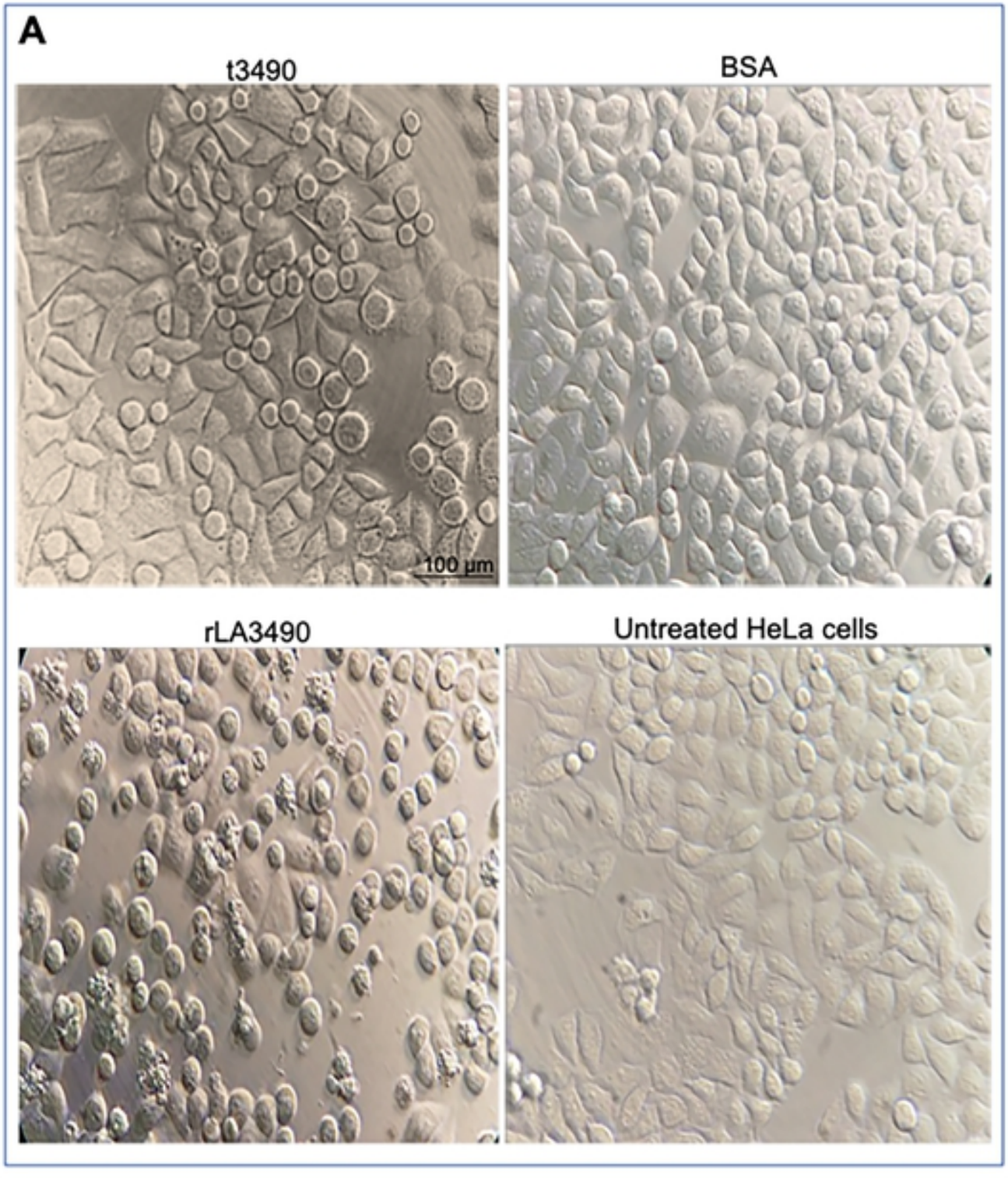
A
t3490
BSA
100 µm
rLA3490
Untreated HeLa cells

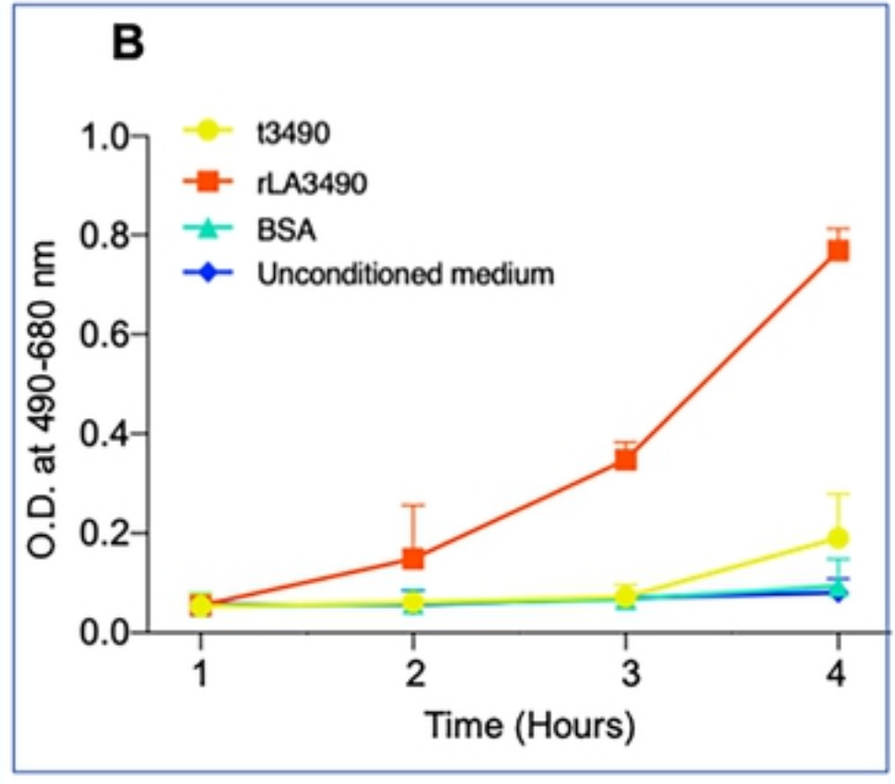
B
t3490
rLA3490
BSA
Unconditioned medium
O.D. at 490-680 nm
1.0
0.8
0.6
0.4
0.2
0.0
1
2
3
4
Time (Hours)

Figure 4

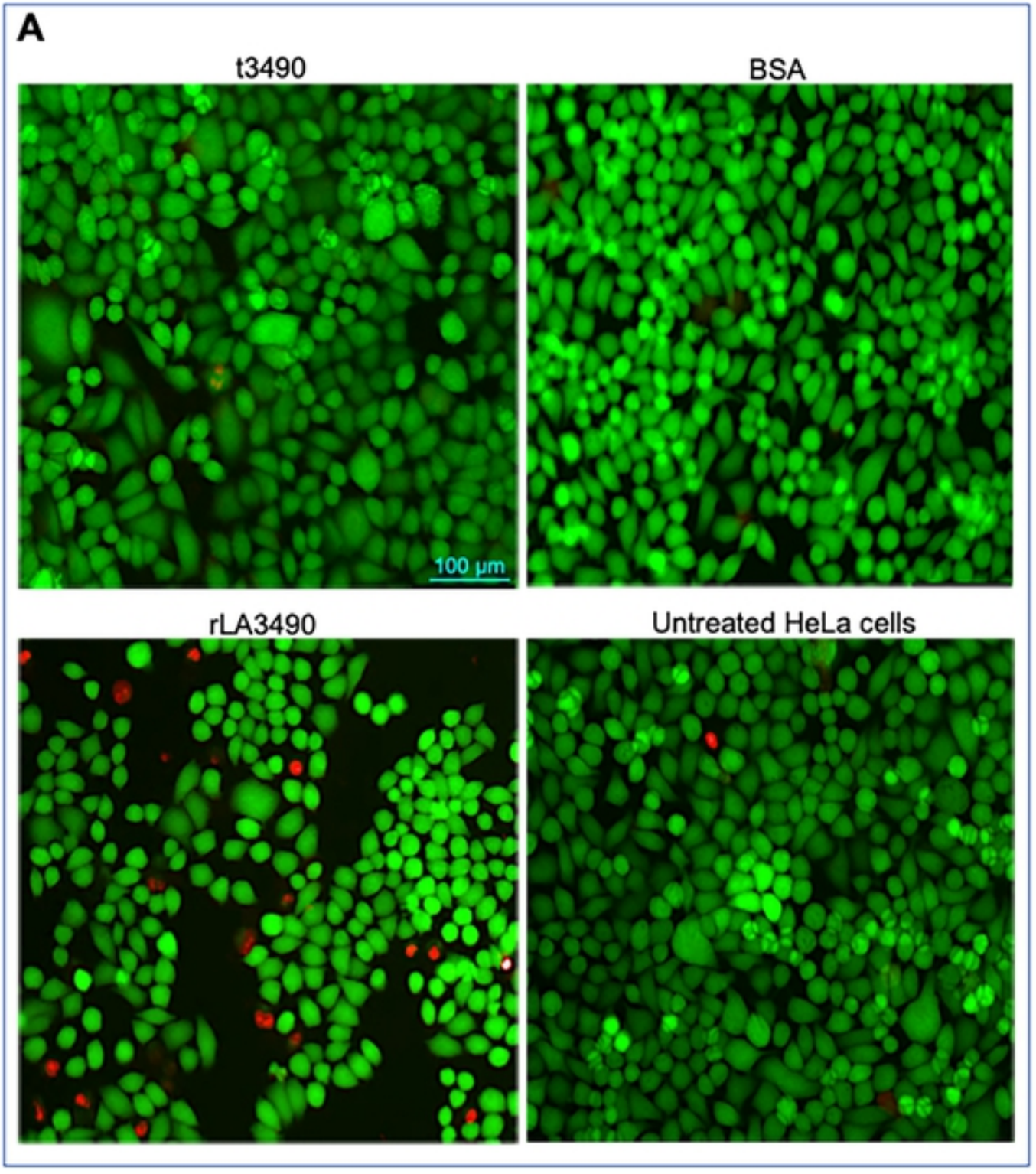
A
t3490
BSA
100 µm
rLA3490
Untreated HeLa cells

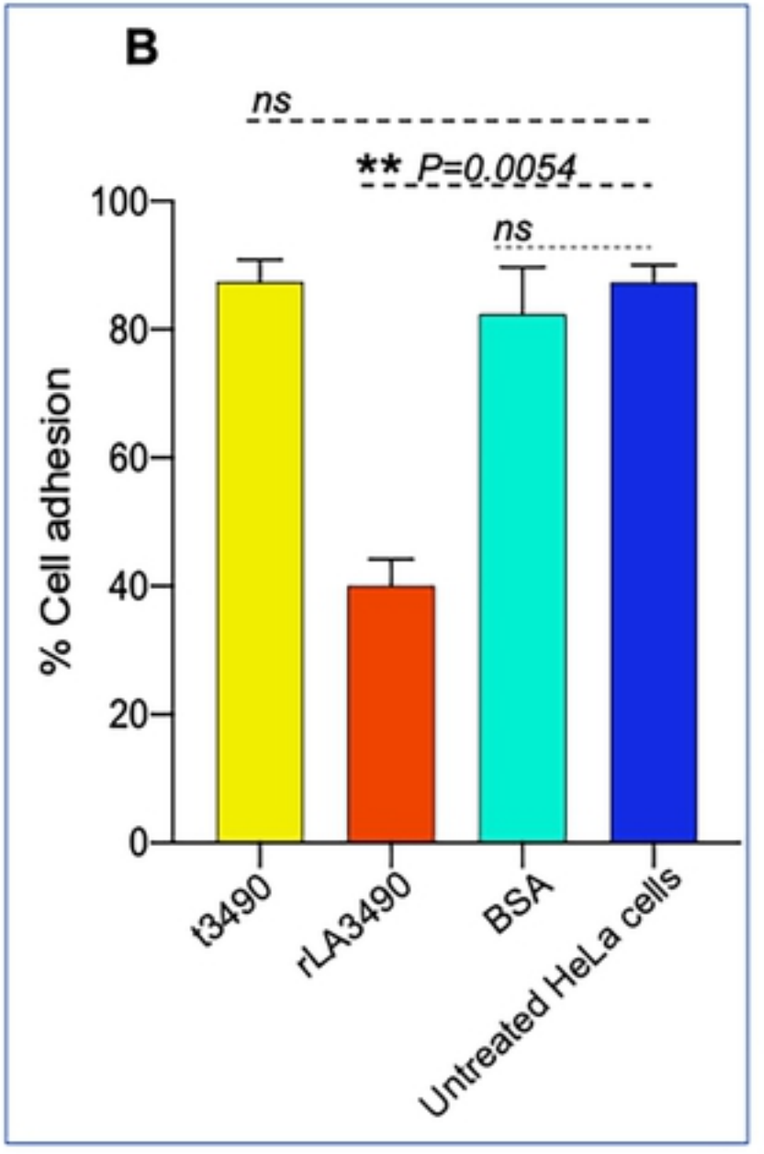
B
ns
** P=0.0054
ns
% Cell adhesion
100
80
60
40
20
0
t3490
rLA3490
BSA
Untreated HeLa cells

Figure 5

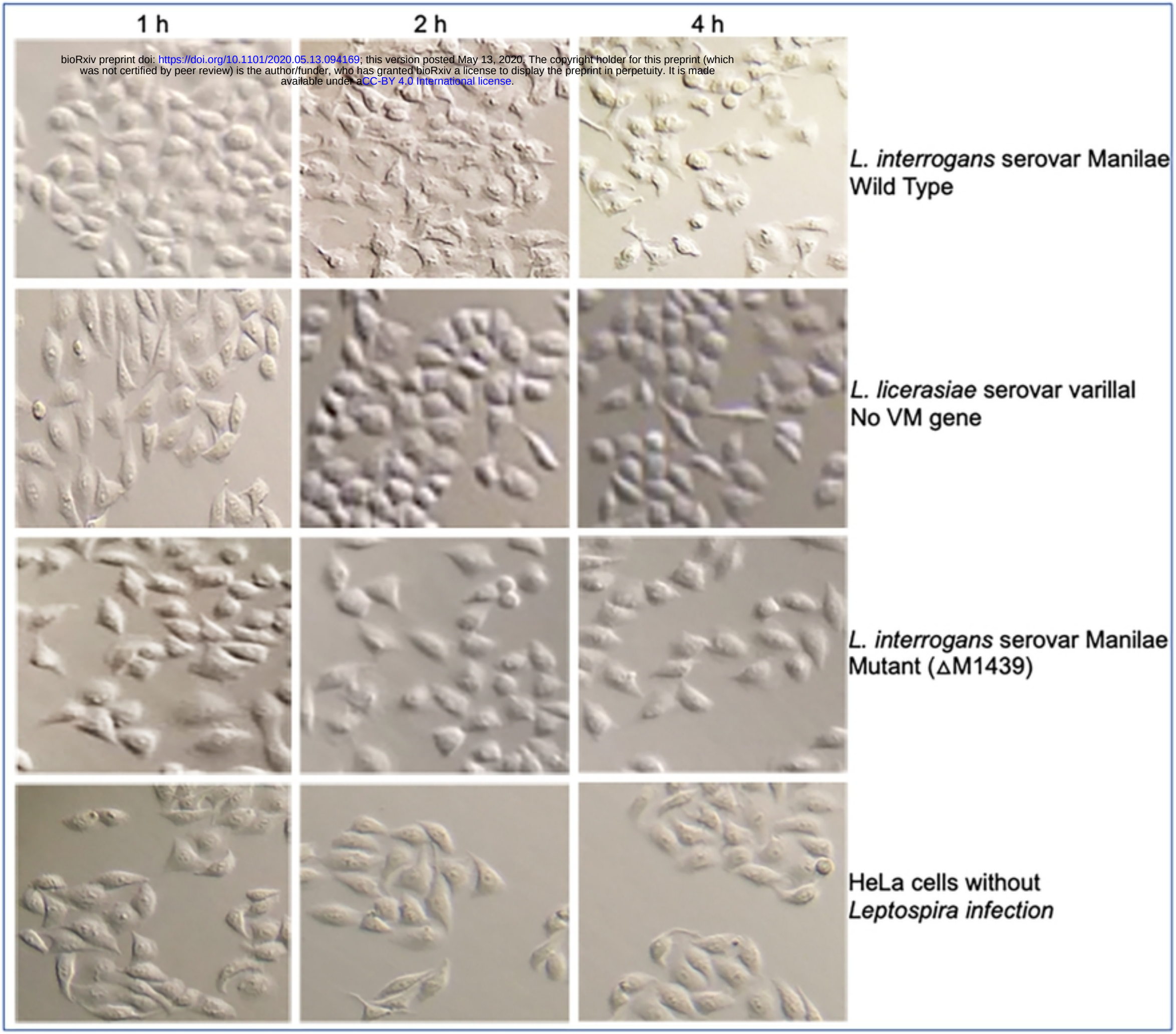

Figure 6

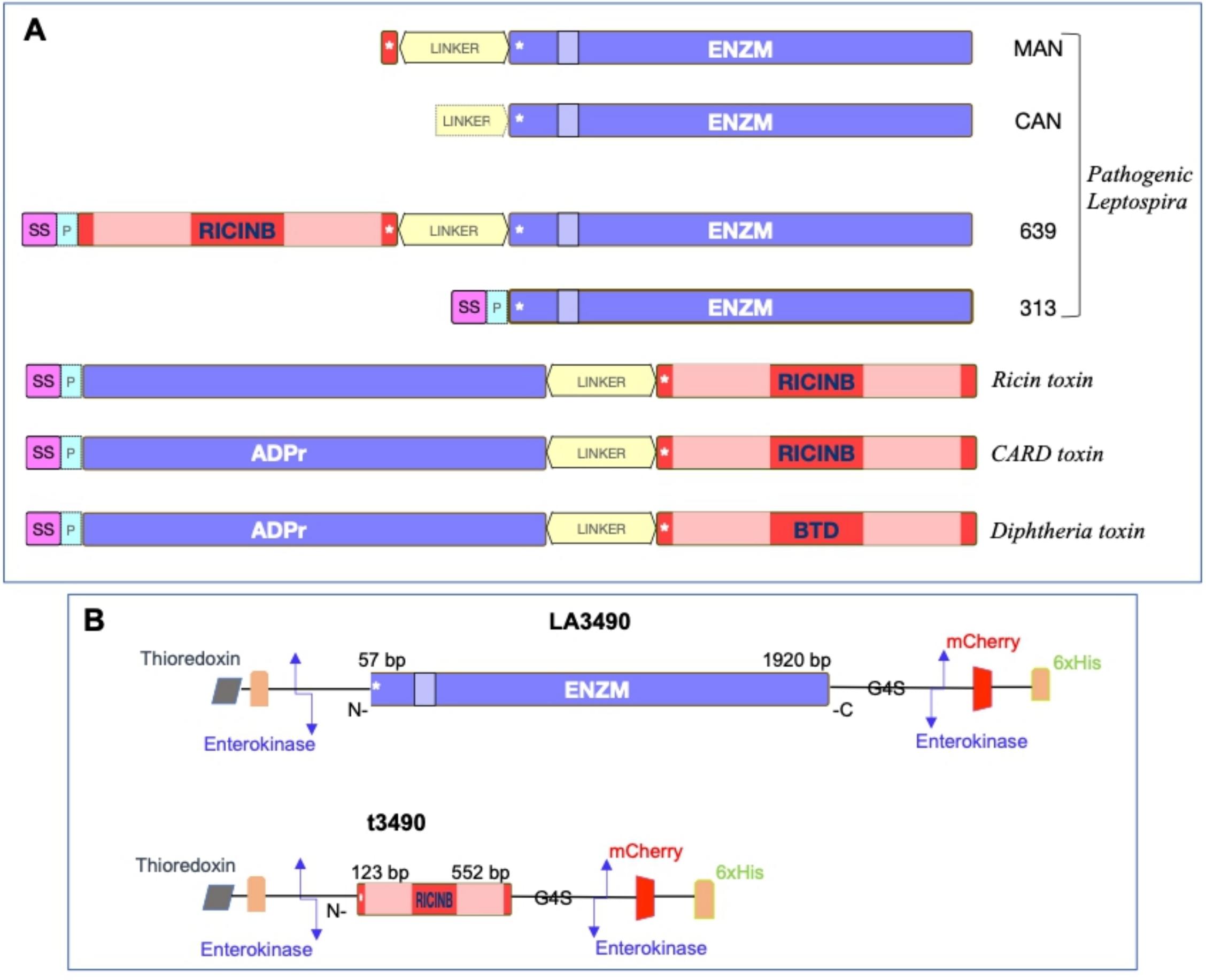

Figure 1

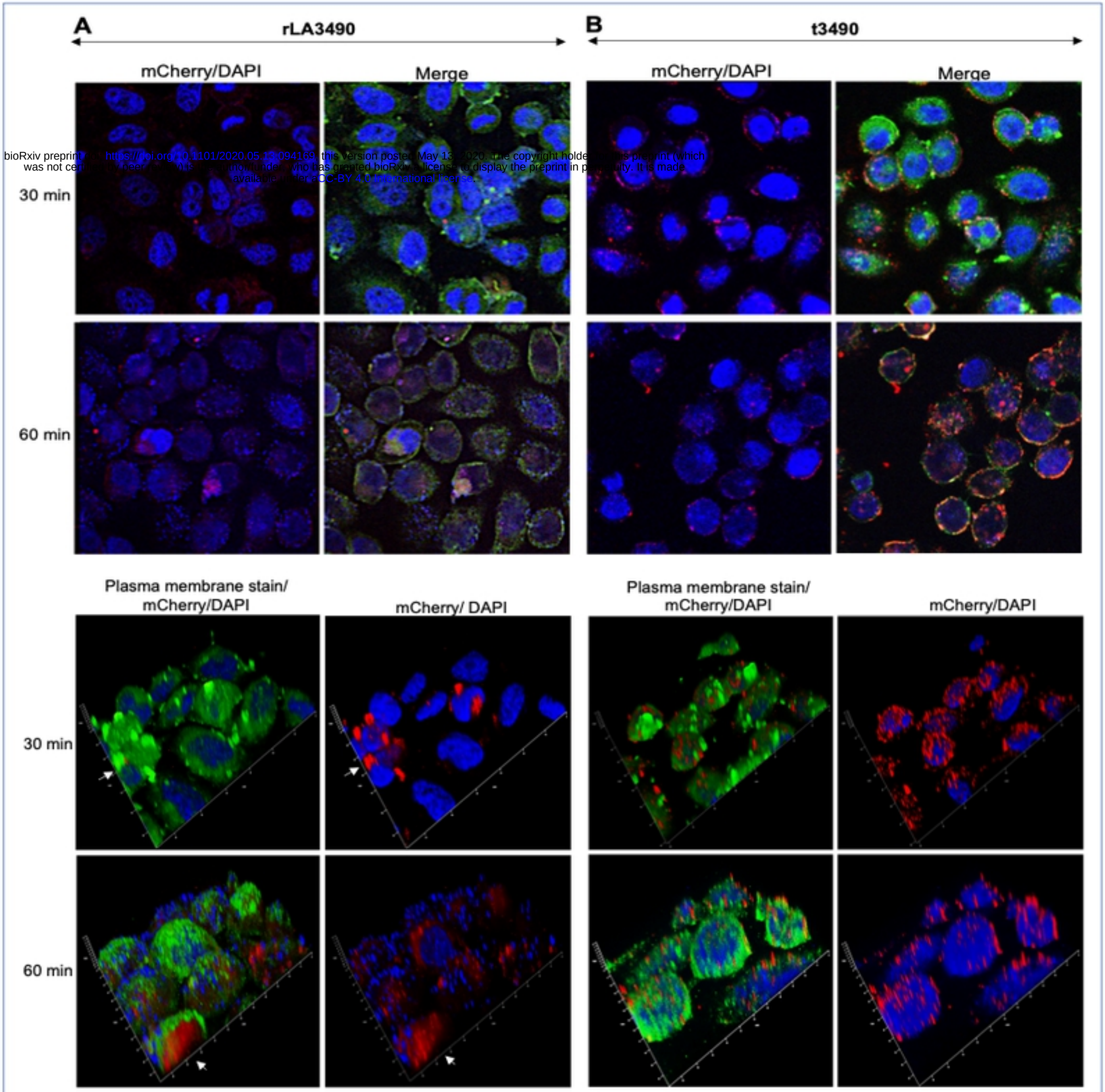

Figure 7

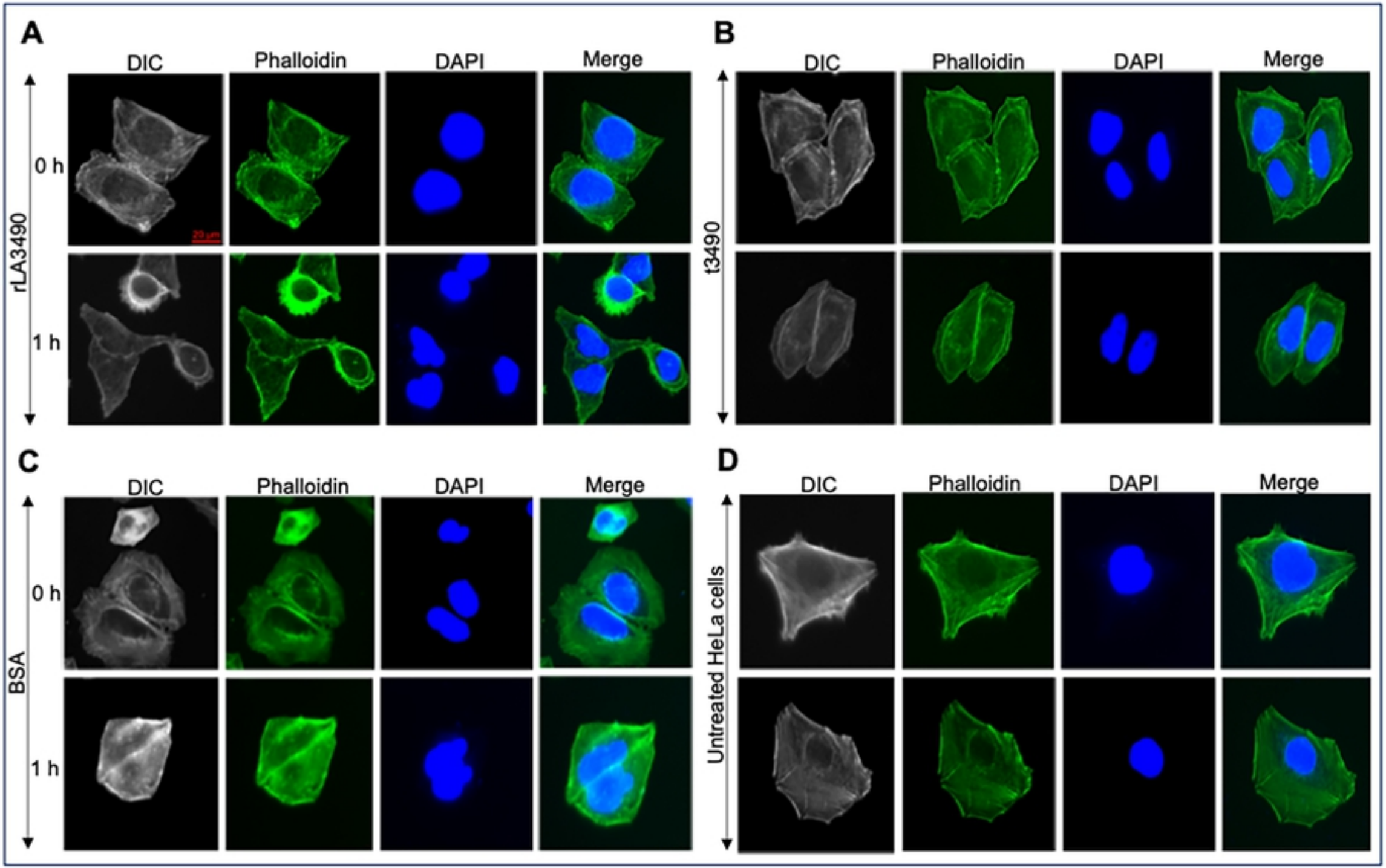
A
DIC
Phalloidin
DAPI
Merge
rLA3490
0 h
1 h
B
DIC
Phalloidin
DAPI
Merge
t3490
C
DIC
Phalloidin
DAPI
Merge
BSA
0 h
1 h
D
DIC
Phalloidin
DAPI
Merge
Untreated HeLa cells

Figure 8